Environ Sci Pollut Res (2016) 23:13342–13354
DOI 10.1007/s11356-016-6502-y

RESEARCH ARTICLE

USPIO assisting degradation of MXC by host/guest-type immobilized laccase in AOT reverse micelle system

Yu-Xiang Yang[1] · Na Pi[1] · Jian-Bo Zhang[2] · Yan Huang[1] · Ping-Ping Yao[1] · Yan-Jie Xi[1] · Hong-Ming Yuan[3]

Received: 29 September 2015 / Accepted: 17 March 2016 / Published online: 29 March 2016

Abstract The laccase and ultrasmall superparamagnetic iron oxide nanoparticles (USPIO) have been assembled inside the tubular mesoporous silica via co-adsorption technology to prepare host/guest-type immobilized laccase, which is applied to degrade methoxychlor (MXC) in aqueous and reverse micelle environments. The effects of various parameters on degradation of MXC were studied. Under the optimum conditions, the degradation rate could reach maximum value of 45.6 % and remain at 20.8 % after seven cycles. Moreover, the addition of small molecular compound 2, 2′-azinobis-(3-ethylbenzthiazoline-6-sulphonate) to the system could greatly improve the degradation efficiency. The MXC degradation process is a first-order reaction, and the activation energy of MXC degradation catalyzed by immobilized laccase (41.46 kJ mol^{-1}) is relatively lower than that catalyzed by free laccase (44.91 kJ mol^{-1}). Based on the degradation products measured by gas chromatograph-mass spectrometer (GC-MS) and nuclear magnetic resonance (NMR), the degradation mechanism of MXC has also been proposed.

Keywords Tubular mesoporous silica · Ultrasmall superparamagnetic iron oxide nanoparticles · Host/guest-type immobilized laccase · Degradation · Methoxychlor

Responsible editor: Gerald Thouand

Electronic supplementary material The online version of this article (doi:10.1007/s11356-016-6502-y) contains supplementary material, which is available to authorized users.

✉ Yu-Xiang Yang
yxyang@ecust.edu.cn

✉ Yan Huang
huangyan@ecust.edu.cn

[1] School of Chemistry and Molecular Engineering, East China University of Science and Technology, Shanghai 200237, China

[2] Department of Environmental Sciences, Peking University, Beijing 100871, China

[3] State Key Laboratory of Inorganic Synthesis and Preparative Chemistry, College of Chemistry, Jilin University, Changchun 130012, China

Introduction

Methoxychlor (MXC) is an organochlorine pesticide developed for the replacement of dichlorodiphenyltrichloroethane (DDT), which is primarily aimed at preventing or destroying pests on crops and domestic animals. Although MXC's solubility is 0.1 mg/L (Butt and Riaz 2010) in water, it does far exceed the Pollutant Discharge Standard set by the World Health Organization (WHO) (0.04 mg/L). Recent studies have shown that MXC can exert toxic effects by changing the pituitary follicle-stimulating hormone (FSH) secretion, affecting reproductive endocrine of male and female.

The degradation of organochlorine pesticides in organic solvents has ever been carried out by Yu's group (Yu et al. 2007) and our group (Yang et al. 2015), but reports are seldom involved in water phase. The fact that MXC in water undoubtedly threatens the health of humans and other mammals, thus biodegradation of MXC is very urgent.

The two-tailed anionic surfactant, bis(2-ethylhexyl)sulfosuccinate sodium salt (AOT), is often used to form reversed micelles without co-surfactant, which acts as reaction medium for a variety of enzymatic reactions. According to Lan et al. (2008), appropriate reversed micelles can increase the electrostatic interaction between the head

group of AOT and the surface of enzyme protein and thus improving the catalytic activity of enzyme.

The flexibility of AOT reversed micelle system offers an opportunity for dissolving the organochlorine pesticides including MXC. If the immobilized enzyme is entrapped in the AOT reversed micellar solution, the enzyme system should be active and stable (Kimura et al. 2004), which could also be applied to degrade MXC. Carvalho and Cabral (2000) considered that AOT can largely influence the enzyme activity; they proposed that the activity and stability of enzyme were higher in anionic surfactants (AOT) than in cationic surfactants (cetyltrimethylammonium bromide (CTAB)). Therefore, the activation of immobilized enzyme toward sparingly soluble organochlorine pesticides in water phase is of great interest. What is more, they also found that the dissolved MXC can easily diffuse to the enzyme active center by the aid of interior aqueous phase of reversed micelle for enhanced degradation of environmental pollutants.

The mesoporous materials (Ispas et al. 2009) are widely considered as an ideal carrier for the immobilized laccase due to its large pore volume, high specific surface area, narrow pore size distribution and continuously adjustable pore size. A particular example can be tubular mesoporous silica (SiO_2-TMs) nanoparticles (Hudson et al. 2008). The assembly of ultrasmall superparamagnetic iron oxide nanoparticles (USPIO) inside the pore channels could enhance the functionality of mesoporous silica (Netto et al. 2013).

Vikesland's study (2007) showed that the particle size and aggregation state of suspension play an important role in the reactivity of magnetic iron oxide toward carbon tetrachloride (CCl_4). Fang et al. (2013) also investigated the activation of persulfate by iron oxide nanoparticles for the degradation of 2,4,4′-CB (PCB28) in aqueous solution. They all found that the magnetic iron oxide with less than 10 nm could generate quantum confinement effects, which can result in altering the surface free energy and increasing the reactivity significantly. But, until now, there is very little research on USPIO-assisted degradation of MXC by immobilized laccase in aqueous medium. Luo and Zhang (2010) successfully prepared magnetic cellulose microspheres for covalent immobilization of penicillin G acylase, leading to highly effective catalytic activity, thermal stability, and enhanced tolerance to pH variations with acceptable reusability and good recovery, mainly due to "magneto-induced effect."

Due to large area to volume ratio, SiO_2-TMs have advantages as a host carrier (Garcia-Galan et al. 2011) to immobilize enzyme. USPIO as guest can not only assist adequate enzyme uniformly immobilized in the host carrier, but also USPIO as a tool serves to modify favorably (also through protein conformational changes) enzyme properties (Secundo 2013), in which, the protein conformational changes are correlated with the size and shape of the nanoscale level of the support. Besides, USPIO has good biocompatibility to complement the structural complexity of enzyme (Chen et al. 2012) and improve stability of the enzyme. Because of special characters and high enantio-selectivity, USPIO has shown broader substrate specificity in enantio-selective hydrolysis of racemic epoxides under mild conditions (Deepthi et al. 2014). Moreover, USPIO particles are also found to have intrinsic catalysis activities and high electron-transferring capabilities (Wang et al. 2014), facilitating greatly improved peroxidase-like catalysis and electrocatalysis activities.

In this paper, the product of magnetic host/guest-type immobilized laccase (laccase-MHGI) was obtained based on the co-adsorption of USPIO and laccase into the pore channels of SiO_2-TMs using cross-linking methods. The effects of different conditional parameters on the MXC degradation in water phase were further discussed. Besides, the reusability and catalytic reaction activation energy were studied and the degradation mechanism of MXC was also speculated according to the degradation products.

Materials and method

Materials

Calcium chloride, sodium carbonate, CTAB, dioctylsulfosuccinate sodium (AOT), polyoxyethylenesorbitan monooleate (Tween 80), absolute ethyl alcohol, tetraethoxysilcane (TEOS), 2′-azino-bis-(3-ethylbenzothiazoline-6-sulfonic acid) diammonium salt (ABTS), ammonia, diphenyl ether, ferric trichloride, ferrous sulfate, oleic acid, oleylamine, anhydrous acetic acid, anhydrous sodium acetate, guaiacol, *n*-hexane, and sodium carbonate (all of analytical grade) were purchased from Shanghai Lingfeng Chemical Reagent Co. Ltd. (Shanghai, China). Ferric acetylacetonate, MXC, and 1,2-hexadecane glycol (AR grade) were supplied by Shanghai TCI Development Co., Ltd. Glutaraldehyde (BR grade) and laccase from Trametes versicolor were purchased from Sigma-Aldrich Co.

Preparation of laccase-MHGI

The SiO_2-TMs and USPIO were prepared by hard template and thermal decomposition methods, respectively, which could be seen in Supplementary Material.

The typical preparation of laccase-MHGI based on the optimal condition in Fig. S1 at room temperature was conducted as below; 20 mg of USPIO was dispersed into 5 mL of 0.05 mol/L AOT/hexane solution to form microemulsion. Into 0.1 mL HAc-NaAc buffer (pH 5.5), 2.5 mg laccase was added and then mixed with microemulsion by ultrasonic treatment. Finally, 0.1 g of SiO_2-TMs was added into the mixed solution as well. After oscillating at 25 °C for 8 h and drying at room temperature overnight, the system was further treated

with 5 mL of glutaraldehyde (6 %) for cross-linking. After oscillating at 25 °C for 8 h again, centrifugating, and washing the product with buffer solution three times, eventually, the laccase-MHGI was obtained and then kept in a refrigerator at 4 °C for further use. The mean weight of immobilized laccase was 110.5 mg after drying in triplicate, while the amount of laccase immobilized on the SiO_2-TMs can be determined by following procedure (Šulek et al. 2011; Han et al. 2015). The recovered activity and relative activity could be calculated according to Eqs. (1) and (2), respectively.

$$\text{recovered activity}(\%) = \text{immobilizedlaccase activity in thenth cycle}/\text{free laccase activity}*100\% \quad (1)$$

$$\text{relative activity}(\%) = \text{immobilizedlaccase activity in thenth cycle}/\text{immobilizedlaccase activity in the1stcycle}*100\% \quad (2)$$

With energy-dispersive spectrometer (EDS) analysis employed, USPIO amount loaded onto the SiO_2-TMs was calculated precisely.

The activity of free and immobilized laccase was spectrophotometrically determined in a reaction medium containing 4 mmol/L guaiacol as substrate in HAc-NaAc buffer (pH 5.0) at 30 °C in the absorbance at 465 nm ($\varepsilon_{465} = 12200\ M^{-1}\ cm^{-1}$). A suitable amount of free and immobilized laccase was added into the substrate solution and immediately stirred. The absorbance of the supernatant was determined using a UV-vis spectrophotometer after 30 min. One unit of enzyme activity (U) is defined as the amount of enzyme required to oxidize 1 μmol of substrate per minute (Tavares et al. 2015; Jiang et al. 2011).

Thermal and operating stability

The thermal stability studies on the free and immobilized laccase were conducted by treating them with 4 mmol/L guaiacol (5 mL) and glutaraldehyde cross-linking in 5 mL of NaAc-HAc buffer solution (pH 5.5) for 30 min at different temperatures. After reaction, the solution was separated using a high-speed centrifuge at 8500 rpm for 1 min; then, 5 mL of the supernatant liquid was taken for the activity measurement immediately.

In order to study the effect of cross-linking agent glutaraldehyde on the activity of immobilized laccase, the immobilized laccase without cross-linking was prepared under the typical preparation process. The operating stability of the immobilized laccase with and without glutaraldehyde was evaluated by continuously carrying out multiple operation cycles with 5 mL of 4 mmol/L guaiacol as substrate at 30 °C, respectively. The solution was separated by centrifugation at the speed of 8500 rpm when each cycle ended, and then, the supernatant liquid was taken for activity measurement as soon as possible. Afterward, the separated immobilized enzyme was washed three times using NaAc-HAc buffer solution (pH 5.5) and repeated with a fresh aliquot of substrate.

Degradation of MXC in aqueous and reverse micelle environments by immobilized laccase

In a typical system of MXC degradation, 0.1 g laccase-MHGI was added into the reaction vessel containing 5 mL prepared mixture of AOT-MXC-buffer solution (pH 5.5, C_{MXC} 25 mg/L, C_{AOT} 4 g/L). The reaction vessel was then placed in model TQZ-312 platform temperature-controlled shaking incubator and kept at 45 °C for 10 h. After that, the reaction mixture was centrifuged to separate the immobilized laccase, and the supernatant was collected and extracted by 5 mL *n*-hexane thrice, and then, all of the three extracted solutions were concentrated by vacuum rotary evaporator. Next, the concentrated residue and 1 mL of 30 $mg \cdot L^{-1}$ octacosane (internal standard)/*n*-hexane were all dissolved in *n*-hexane to 5 mL; finally, 1 μL samples were subsequently subjected to gas chromatograph (GC) analysis. By measuring the peak-area ratio of A_{MXC}/As, the concentration of MXC (C_{MXC}/mg L^{-1}) could be obtained in Eq. (3), which can be derived from standard curve (Fig. S3).

$$C_{MXC} = 66.9(A_{MXC}/\text{As}) + 0.565 \quad (3)$$

Each group of experiments was manipulated in triplicate, and the arithmetic mean values were counted, with the standard deviations less than 3 %.

The calculation of MXC degradation rate

The concentration of MXC was calculated with internal standard method, and its standard curve could be seen in Fig. S3. In the degradation process of laccase-MHGI,

the carrier SiO_2-TMs would absorb part of MXC owing to its large specific surface area. In order to calculate degradation rates, the adsorption amount of MXC on the cross-linked SiO_2-TMs must be determined. The MXC removal rates, the adsorption rates, and the degradation rates were calculated by Eqs. (4), (5), and (6):

$$\text{adsorption rate}/\% = (C_0 - C_a)/C_0 * 100\% \quad (4)$$

$$\text{removal rate}/\% = (C_0 - C_d)/C_0 * 100\% \quad (5)$$

$$\text{degradation rate}/\% = (C_a - C_d)/C_0 * 100\% \quad (6)$$

where C_0 and C_d were the MXC concentrations before and after degradation by immobilized laccase, respectively; C_a was the concentration of MXC after adsorption of blank carrier.

Determination of MXC degradation intermediates

To determine the degradation intermediates of MXC, five copies of degradation experiments were performed under the best conditions. Then, the five separated supernatants were collected together and extracted by 25 mL of *n*-hexane thrice. Finally, all of the three extracted solutions were combined and dried by anhydrous Na_2SO_4. After that, they were vacuumly concentrated to 5 mL and subjected to gas chromatograph-mass spectrometer (GC/MS) analysis.

The intermediates formed during MXC degradation were identified by GC/MS (Agilent Technologies). It is composed of a 7890A GC equipped with a 7683B series injector and a 5975C mass spectrometer in EI mode at 70 eV. The analyses were made by splitless (0.7 min) injection, and the mass spectra (*m*/*z*) were given in Table 1. The nuclear magnetic resonance (NMR) measurements were performed on a Bruker Avance III 600-MHz NMR spectrometer (Rheinstetten, Germany) at 600 MHz for 1H nuclei and 150 MHz for 13C nuclei. TMS was used as an internal standard for NMR analysis, and the chemical shift values (ppm) are given in Table 2.

Results and discussion

Characterization of SiO_2-TMs and laccase-MHGI

The small-angle X-ray diffraction (SXRD) pattern of SiO_2-TMs is shown in Fig. S2a. It exhibited a diffraction peak at $2\theta = 2.88°$ in 1~10° range, corresponding to the crystal plane (100), demonstrating that the material had ordered hexagonal pore structure (Shao et al. 2009).

Figure S2b shows nitrogen/stripping absorption isotherm and pore size distribution of SiO_2-TMs. The isotherm was in line with the IV type absorption isotherm possessing the character of typical mesoporous materials. Due to nitrogen molecules in the capillary condensation in the mesoporous channel, a clear hysteresis loop of H1 type can be observed. It indicated that the ordered mesoporous structure of the sample was consistent with small-angle XRD characterization results in Fig. S2a. Besides, the nitrogen adsorption/desorption experiments showed that the measured Brunauer-Emmett-Teller (BET) surface area was 843.21 m^2/g while the Barrett-Joyner-Halenda (BJH) pore volume and the most probable pore diameter were 0.55 cm^3/g and 3.28 nm, respectively.

The morphology and microscopic structure of SiO_2-TMs, USPIO, and laccase-MHGI were characterized using transmission electronic microscopy (TEM). The TEM image of SiO_2-TMs recorded in Fig. 1a clearly exhibited a uniform tubular structure with length in the range of 2.5~6.8 μm and pore diameter in the range of 0.6~1.3 μm. As shown in Fig. 1b, c, the USPIO had a mean particle size of 5.5 nm with a well dispersion; after co-adsorption of laccase and USPIO into tubular channel of SiO_2-TMs followed by glutaraldehyde cross-linking, the laccase-MHGI (Fig. 1c) still exhibited tubular structure with a length of about 4.5~7.3 μm and a diameter of 1.2~1.6 μm, inside which 293~631 nm laccase-adsorbed USPIO particles were found to be uniformly dispersed, besides some of laccase-adsorbed USPIO particles distributed around the tubular channel. The findings demonstrate that laccase and USPIO are co-assembled to form new adsorbed USPIO particles.

The high-resolution transmission electronic microscopy (HRTEM) image recorded in Fig. 1d showed grayish-black dots about 8~10 nm uniformly dispersed in tubular channel,

Table 1 Mass spectra data of products after degradation of MXC

Products	Mass spectrum *m*/*z* (relative intensity)
1-(2,2-Dichloro-1-phenyl-ethyl)-4-methoxy-benzene (I)	281 (9.6), 207 (6.4), 112 (2.9), 98 (7.0), 83 (22.2), 70 (26.3), 57 (100), 41 (34.1), 31 (18.8), 28 (47.8)
Cyclohexane (II)	84 (79.6), 69 (36.2), 56 (100), 41 (50.5), 28 (6.4), 15 (1.4)
Methyl cyclopentane (III)	84 (15.6), 69 (55.2), 56 (100), 41 (51.5)
4-(2,2-Dichloro-ethyl)-1-methoxy-cyclohexene (IV)	211 (20.4), 184 (1.5), 112 (64.9), 99 (30.9), 83 (33.0), 70 (100), 57 (69.9) 41 (34.0), 28 (9.4)
2-Methylpentene (V)	84 (15.6), 69 (55.2), 56 (100), 41 (51.5), 27 (12.1), 15 (1.1)

Table 2 1H-NMR and 13C-NMR results of MXC degradation product by laccase-MHGI

Chemical shift (δ) (ppm)	
^{1}H-NMR	^{13}C-NMR
0~2 ($-CH_3$, $-CH_2$-, $-CH-$)	10~50 ($-CH_3$, $-CH_2$-, $-CH$-, $-CH(C_6H_5)(C_6H_5OCH_3)$)
3~5 ($CH_2=CR_1R_2$, $R_1R_2C=CH$-, $-OCH_3$)	70~80 ($-CH_2Cl$, $-OCH_3$)
6.0~6.5 ($-CHCl_2$)	100~110 ($CH_2R_1R_2$)
7~8 ($-C_6H_5$)	130~140 ($-C_6H_5$)

indicating that the USPIO were present in the pore channel of the tubular sample, probably because the USPIO particles have space regulation ability, inducing co-adsorbed particle uniform dispersion.

Recovered activity and stability of immobilized laccase

According to Šulek et al. (2011) and Han et al. (2015), the recovered activity of laccase immobilized on SiO_2-TMs can be determined, with the results shown in supplemental Table S1. Besides, the EDS determination of the Fe loaded on SiO_2-TMs can be seen in Fig. S4.

From Table S1, it is found that the recovered activity of laccase was 43.40 % after immobilization. As for USPIO, the loading amount was calculated as 9.491 mg by the average amount of immobilized laccase multiplied by (M_{Fe3O4}/M_{3Fe}) and loading percentage of Fe showed in Fig. S4. The total amount of USPIO before immobilization was 20 mg, whose loading percentage was thus calculated as 47.46 %.

Activities of free and immobilized laccase were compared at different temperatures in Fig. 2a. Although activities of both enzymes depended significantly on temperature, the immobilized enzyme had a relatively wider functioning range of temperature than free laccase. The optimum temperature for the free laccase to function was 35 °C; by comparison, immobilization increased stability of the enzyme with enhanced thermal stability, so the optimum temperature for the laccase-MHGI was transferred to a higher temperature of 45 °C, with the maximum value reaching 1840.2 U/g. When the temperature reached over 45 °C, nearly 67 % of the activity for immobilized laccase can be observed, while most free laccase became inactive. This can be explained as follows: as one type of protein enzyme, laccase is temperature-sensitive and liable to be denatured, due to the conformational changes of laccase and the oxidation of labile groups. However, when immobilized by cross-linking with glutaraldehyde, the laccase was located inside the pore channels of SiO_2-TMs, accompanied with adsorption of nano-Fe_3O_4, as shown in Fig. 1. So, the laccase was protected by the SiO_2 channel shell, and the cross-linking of glutaraldehyde would increase the stability of laccase inside the pore channels due to the binding interaction between laccase and SiO_2-TMs (Wang et al. 2012).

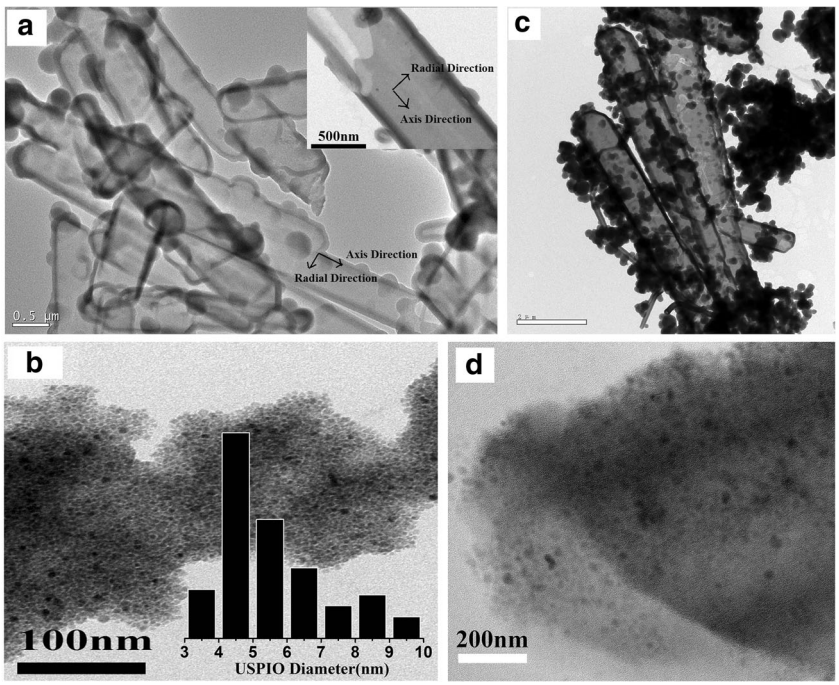

Fig. 1 TEM and HRTEM image of SiO_2-TMs, USPIO, and laccase-MHGI. **a** SiO_2-TMs, **b** USPIO, and **c**, **d** laccase-MHGI

As a result, the structure of laccase became stable and difficult to change even at a high temperature. Thus, the thermal stability of laccase-MHGI increased.

As seen from Fig. 2b, the operating stability of free and immobilized laccase could be measured by their recovered activities after repeated use. The recovered activities of immobilized laccase with and without glutaraldehyde cross-linking were found to be 43.40 and 67.07 %, respectively. It might be that covalent attachment was often coupled with the decrease of adsorption capacity and activity recovery during the cross-linking process. However, after 2 cycles of oxidizing by guaiacol, the recovered activities of immobilized laccase without glutaraldehyde cross-linking were reduced to 14.87 % sharply and reached 5.06 % after 7 cycles. On the contrary, the relative activities of immobilized laccase with glutaraldehyde remained near 81.94 % of its initial activity and at 42.47 % after 7 recycles, indicating reusability of the laccase immobilized onto SiO_2-TMs with glutaraldehyde cross-linking, which had a stronger binding interaction than that without cross-linking.

The optimum conditions of the MXC degradation by laccase-MHGI

To increase the degradation efficiency of MXC, an organic heterogeneous medium of AOT reversed micelles has been tried (AOT is a two-tailed surfactant, and it is easy to form a reversed micelle without co-surfactant) (Zhang et al. 2006). In this paper, the anionic surfactant AOT, the cationic surfactant CTAB, and the nonionic surfactant Tween 80 were selected to investigate the degradation of MXC with laccase-MHGI. The results could be seen in Fig. 3a. The degradation system with AOT displayed the most excellent degradation ability (44.3 %); in contrast, the addition of CTAB and Tween 80 resulted in lower degradation rates at 12 and 9.1 %, respectively. In the presence of CTAB or Tween 80 system, emulsifying phenomenon was so serious during the extraction of degraded products that it made the separation and measurement difficult; thus, the degradation rate was lower than that of AOT system.

In order to explore the specific effect of AOT on the degradation of MXC, a set of experiments was performed under different concentrations of AOT (Fig. 3b). It can be found that both the removal rate and the degradation rate increased firstly with an increase in level of AOT and then decreased, reaching the maximum values of 51.8 and 44.3 % at 4 g/L, respectively. Since an increase of AOT concentration enhanced the number of micelles and micelle volume, the solubilization capacity of MXC would be enlarged. However, an excess of AOT might change the existence state of AOT molecules in the system, forming complex polymers instead, which influenced individual solubilization effect on the solubility of MXC. A set of experiments have been designed to demonstrate these solubilization principles of AOT; the results are shown in Fig. S5b.

The findings showed changes of the solubility of MXC arising from the concentration of AOT in water phase. When the concentration of AOT was less than 4 g/L, the solubility of MXC increased with an increase of AOT concentration, but higher AOT concentration (over 4 g/L) led to solubility of MXC unchanging; it would made specific activity of immobilized enzyme decrease instead (Fig. S5a). Because an excessive AOT may block the mesoporous tubular channel, hinder the admittance of a substrate to enzyme active site, and lead to a decrease of the enzyme activity. When the AOT concentration was controlled at 3~4 g/L, the specific activity of immobilized enzyme reached maximum value of 1829.2 U/g, which was consistent with the results of Fig. 3b. The findings also showed that lower AOT concentration than 3 g/L would not be beneficial to specific activity of immobilized enzyme (Fig. S5a).

Figure 3c indicates that the degradation rate of MXC was 45.15 % when initial concentration was 25 mg/L, higher than 27.43 % for initial concentration 10 mg/L and 9.45 % for 50 mg/L. When substrate concentration inside the tube mesoporous silica decreased to a certain level, the removal rate could be primarily attributed to the degradation rate. But,

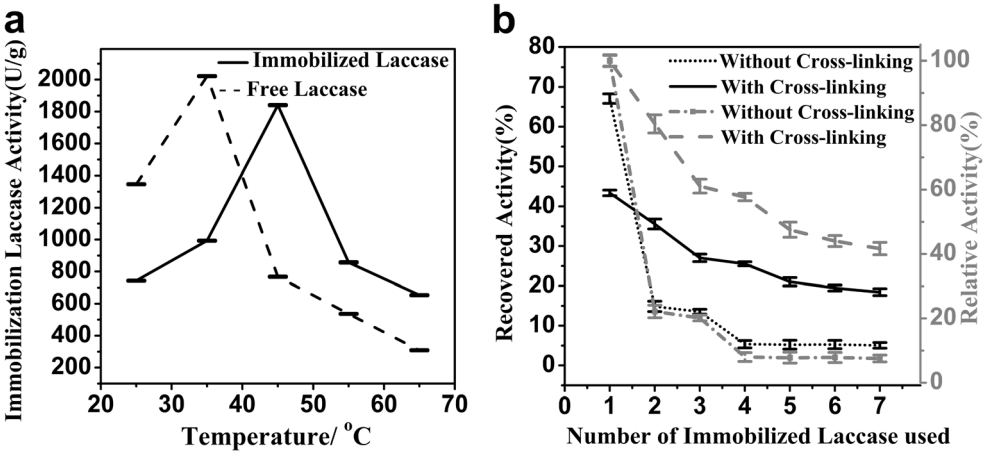

Fig. 2 Thermal stability and operating stability of free and immobilized laccase, the standard deviations less than 3 %. **a** Thermal stability. **b** Operating stability

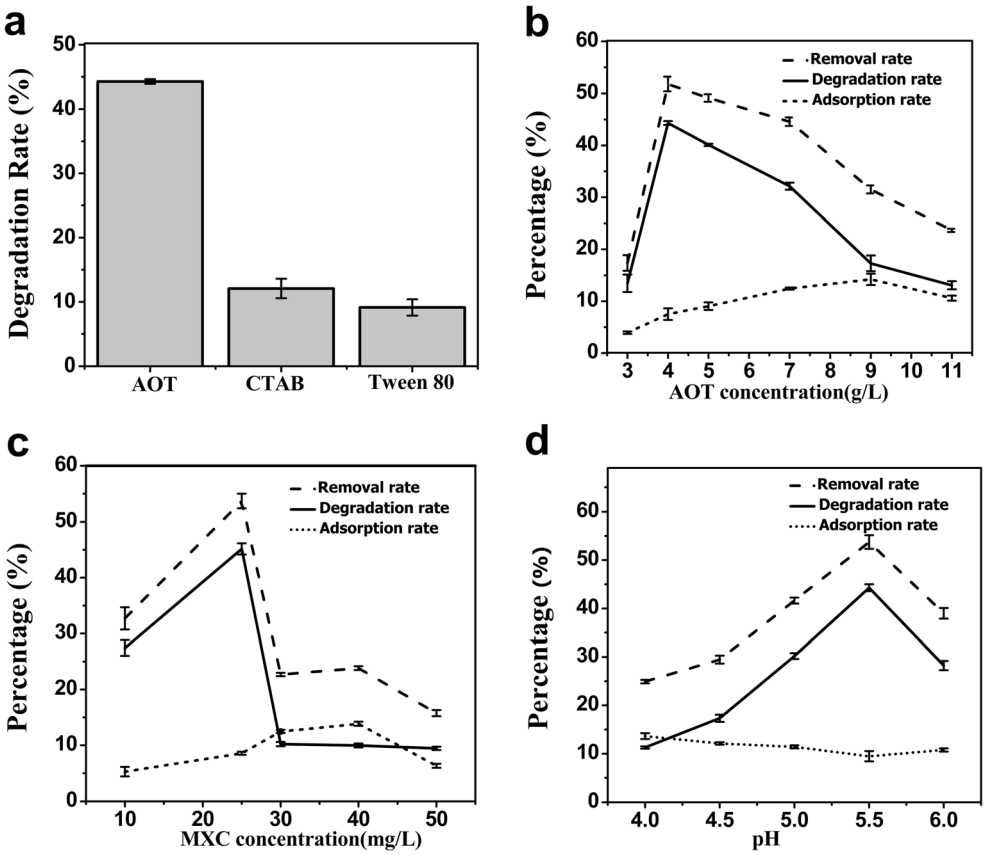

Fig. 3 Effects of various factors on the degradation of MXC by immobilized enzyme, the standard deviations less than 3 %. **a** Different surfactants on the degradation of MXC by immobilized enzyme, with the conditions MXC 25 mg/L, USPIO 6 g/L, pH 5.5, and 45 °C. **b** Various AOT concentrations, with the conditions MXC 25 mg/L, USPIO 6 g/L, pH 5.5, and 45 °C. **c** Various MXC concentrations, with the conditions of USPIO 6 g/L, pH 5.5, and 45 °C. **d** Various pHs, with the conditions USPIO 6 g/L, AOT 4 g/L, MXC 25 mg/L, and 45 °C

when the concentration of MXC was higher, the number of active sites available was covered by the MXC molecules due to their competitive adsorption on the catalytic surface, which blocked direct contact between enzyme and substrate, leading to a relative higher adsorption rate.

To illustrate this fact, the residue MXC remaining on the surface of immobilized enzyme was extracted with *n*-hexane thrice and then concentrated to 5 mL by vacuum. Whereafter, 1 μL samples were subjected to GC analysis immediately; the results can be seen in the Table S2.

According to Table S2, we found that about 8~9 % of non-degraded MXC converged on the surface of immobilized enzyme, which would cause space steric hindrance to obstruct the direct contact between the substrate and laccase. All these factors would result in a decrease of the degradation rate.

The effect of pH on the degradation of MXC using laccase-MHGI was investigated within the pH range of 4.0~6.0 (Fig. 3d). The degradation and removal percentage of MXC increased with increase of pH and then decreased after reaching their maximum value at pH 5.5, indicating that the degradation of MXC was sensitive to the change of pH. Furthermore, the optimum pH range for the degradation of MXC by laccase was related to chemical structure of the substrate. The results were in agreement with the study that the optimum pH range was beneficial to substrates releasing H^+, forming many anions and catalyzing the dechlorination of chloro-aromatic ring by immobilized laccase (Huang et al. 2014).

Figure 4 shows that when the initial concentration of MXC was 25 mg/L, within the temperature range of 30~50 °C, the degradation rate of MXC catalyzed by immobilized enzyme and free enzyme all increased with the extension of reaction time and the rise of temperature firstly. The degradation rate catalyzed by free enzyme achieved its maximum of 53.52 % when the temperature was kept at 35 °C. By this token, MXC could be degraded by immobilized laccase in a wider temperature range. Unfortunately, the degradation rate of MXC by free enzyme almost stopped growing at 45 °C, while the degradation rate catalyzed by immobilized enzyme continued to increase by 17.68 % and reached its maximum of 45.72 %. The results indicated that thermal stability of immobilized enzyme could be improved greatly after immobilization, demonstrating that the free laccase has higher sensitivity to temperature than the immobilized enzyme. Although the motion of molecules became violent in high heat conditions, inducing faster degradation correspondingly, higher temperature would cause the inactivation and denaturation of enzyme, which can be observed in that the degradation rate of MXC by free enzyme declined faster than that of immobilized enzyme under 50 °C in Fig. 4d.

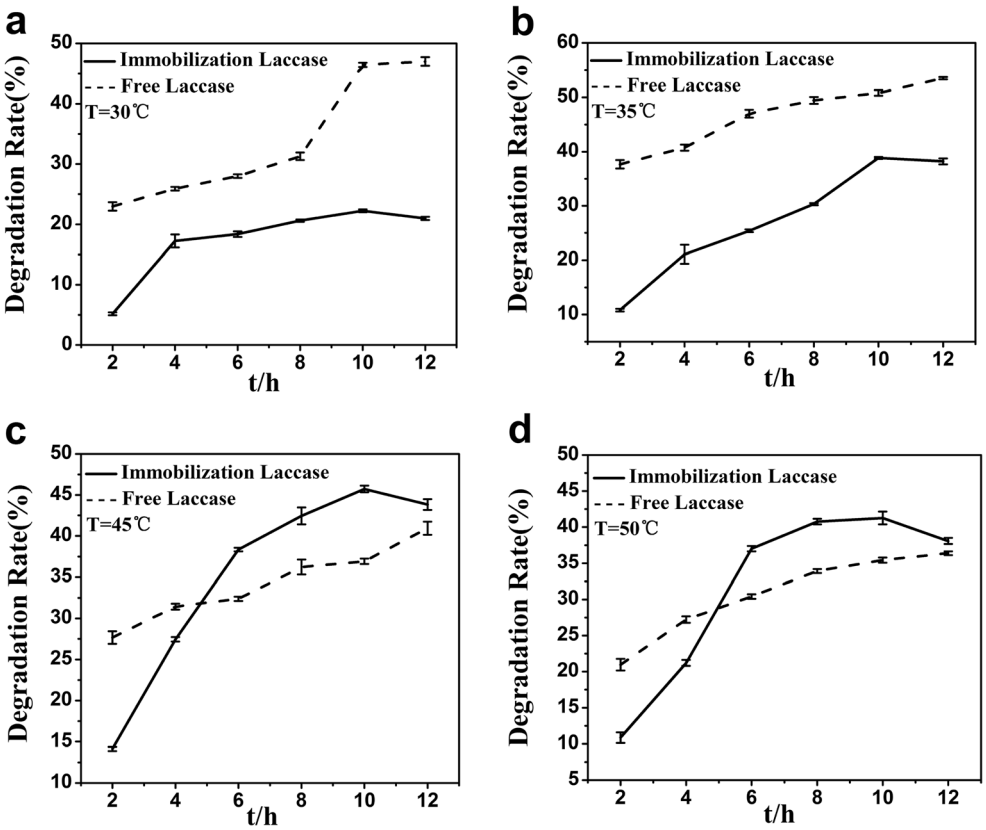

Fig. 4 Effects of temperature and reaction time on the degradation of MXC by free enzyme and immobilized enzyme, the standard deviations less than 3 %

As shown in Fig. 5a, with the continuous increase of USPIO concentration to 4 g/L, the degradation rate gradually increased up to a maximum of 43.73 %, whereas degradation rate showed a decline in its activity when USPIO concentration exceeded 6 g/L. Conformational changes and a better spatial orientation of laccase molecules (Kouassi et al. 2005) are put forward for the reason of USPIO-associated enhancement of the activity of enzyme, because co-adsorption of laccase on appropriate amount of USPIO affects their three-dimensional conformation via specific and nonspecific interactions with USPIO particles such as electrostatic, hydrogen bonding, and hydrophobic interactions (Wu et al. 2009). In contrast, an excess of USPIO loading might block the tubular mesoporous channel and hinder the admittance of a substrate to enzyme active site, leading to the reduction of the enzyme activity and degradation rate (Martel 2015). Therefore, the optimal amount of USPIO was confirmed to be 4 g/L for MXC degradation.

Studies have indicated that the effect of MXC degradation by laccase alone was poor because of the low redox potential of laccase. However, some compounds with small molecular weights can function as electron shuttles once oxidized by the laccase to stable radicals, which oxidize other compounds that are, in principle, not substrates of laccase. Artificial mediators, such as ABTS and violuric acid (VLA), have been verified to enhance the removal efficacy of organic chlorides. For example, under the action of 2,2′-azinobis-(3-ethylbenzthiazoline-6-sulphonate) (ABTS), 40~70 % of phenol could be removed by laccase (Duran and Esposito 2000).

After added ABTS, the color of the MXC degradation system was still brown and gray (Fig. S7). In order to study the role of ABTS in process of MXC degradation, the ABTS aqueous solution was added to the typical system for MXC degradation under the optimal conditions, and the results obtained are shown in Fig. 5. As shown in Fig. 5b, the degradation rate of MXC before and after adding ABTS was 45.71 and 51.12 %, respectively. Through the calculation, the degradation efficiency could be improved by 11.84 % after adding ABTS. In virtue of the low oxidation-reduction potential of laccase, an appropriate amount of ABTS added into the system could be used as mediating agent to transfer electrons, enhancing the capacity of the oxidation of laccase. But, an excess of ABTS would react with laccase to hinder the degradation of MXC, leading to the degradation rate decreasing rapidly, which was also proved by Ren and co-workers (Bourbonnais and Paice 1992). As a result, the optimum ABTS concentration was chosen as 0.7 mmol/L (Fig. 5c).

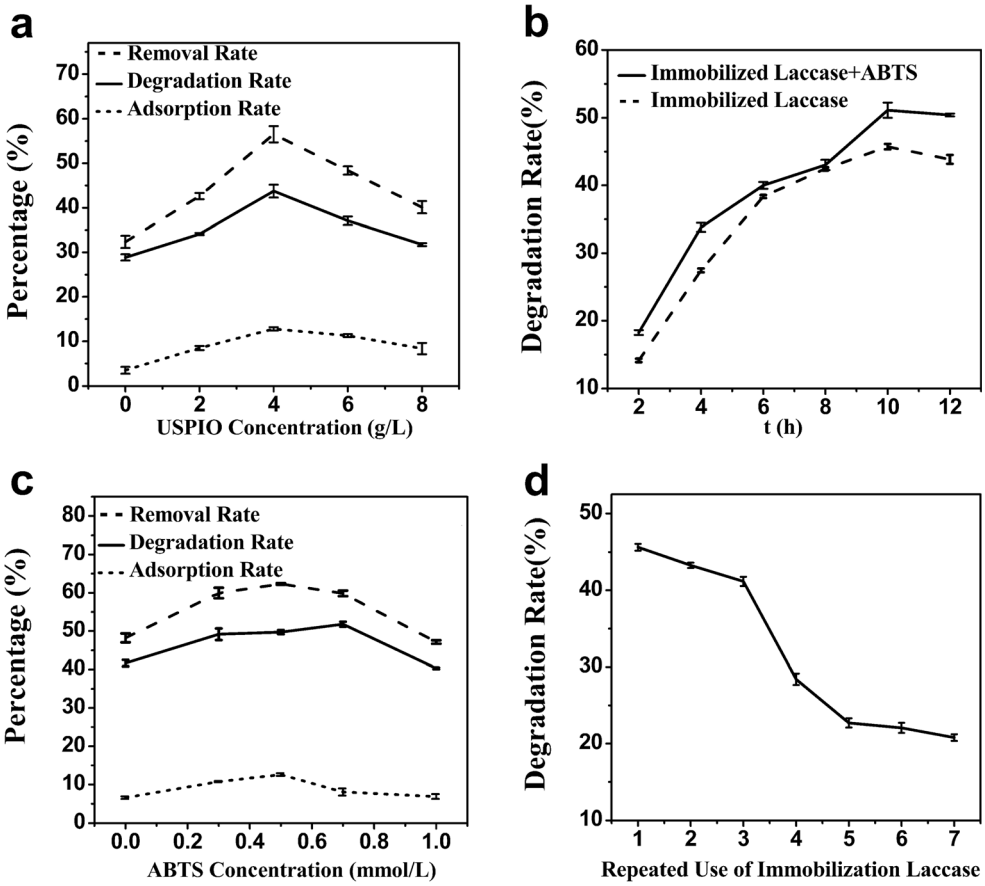

Fig. 5 Effects of USPIO, ABTS, and number of repeated cycles on the degradation of MXC by immobilized enzyme, the standard deviations less than 3 %. **a** Various USPIO, with the conditions, AOT 4 g/L, MXC 25 mg/L, 45 °C, and pH 5.5. **b** The influence of ABTS on the degradation of MXC by immobilized enzyme. **c** Various ABTSs, with the conditions USPIO 6 g/L, AOT 4 g/L, MXC 25 mg/L, 45 °C, and pH 5.5. **d** Number of repeated cycles, with the conditions USPIO 6 g/L, MXC 25 mg/L, pH 5.5, AOT 4 g/L, and 45 °C

Degradation activation energy of laccase to MXC

The MXC degradation dynamics curve of laccase in aqueous phase under different temperatures were found to follow the first-order reaction as shown in Eq. (7):

$$C_t = C_0 \exp(-kt) \tag{7}$$

where C_0 is the initial concentration of reactant, C_t is the concentration of reactants at time t, and k is the first-order reaction rate constant. The activation energy of MXC degradation catalyzed by free laccase and laccase-MHGI could be determined according to the Arrhenius equation in Eqs. (8) and (9) in Fig. S8, respectively.

$$\ln k = -5402.0512/\mathrm{RT} + \mathrm{B} \tag{8}$$

$$\ln k = -4987.18/\mathrm{RT} + \mathrm{B} \tag{9}$$

As a result, the activation energy of the typical reaction catalyzed by native laccase and laccase-MHGI was calculated to be about 44.91 and 41.46 kJ/mol, respectively.

In contrast to free laccase, the activation energy catalyzed by immobilized laccase was lower, demonstrating that USPIO had special effects on laccase degradation because of the "magnetic effect" (Huang et al. 2014), which promoted the degradation of MXC by laccase in water phase. Besides, when the activation energy was less than 100 kJ/mol, the degradation reaction could take place just by slight heating. Therefore, MXC degradation reaction catalyzed by free laccase or immobilized laccase could come up at room temperature without heating in water phase.

The reusability of immobilized laccase

Magnetic bio-separation technology is a promising strategy for the preparation of immobilized enzymes on USPIO, as it can be easily recovered using an external magnetic field and recycled for iterative uses. The properties of the composite system with an analogous system in absence of USPIO are compared in Fig. S6. The magnetic properties of USPIO and laccase-MHGI were studied by vibrating sample magnetometer (VSM) at room temperature. As illustrated in Fig. S6a, the saturation magnetization of USPIO and laccase-MHGI was 41.53 and 10.84 emug^{-1}, respectively. Because of the shielding effect of tubular mesoporous SiO_2 shell (host), the magnetic response obviously decreased after coating with silica. However, laccase-MHGI could be easily separated by using a magnet within 5 min (Fig. S6b).

Besides, effects of the reusability of laccase-MHGI on MXC degradation can be found in Fig. 5d. The degradation rate of MXC catalyzed by laccase-MHGI was about 46 %

under optimum conditions. When the regenerated immobilized laccase was used a second time, the degradation rate would decrease to 43 %. With the number of cycles of laccase-MHGI increasing, the degradation rate of MXC decreased gradually. When the number of cycles reached 7, the rate of degradation of MXC still remained at 20.8 %. Compared with the free laccase, the reusability of immobilized laccase was improved markedly. This fact can be explained that MXC can easily diffuse into the mesoporous channels of supports, leading to MXC more easily being degraded by the immobilized laccase.

Studies on degradation reaction mechanism of MXC by immobilized laccase in water phase

Dec and Bollag (1994) proposed that the dechlorination reaction was promoted not only by various oxidoreductases but also by inorganic catalysts. There were three kinds of pathway in the MXC degradation by laccase-MHGI, and the first degradation process was the reductive elimination of chloride and then elimination of methoxyl group under laccase combined with reduction of USPIO, forming the degradation intermediate 1-(2,2-dichloro-1-phenyl-ethyl)-4-methoxy-benzene (I) (*m*/*z* = 281). Li et al. (2012) found that the dechlorinated organic compounds were easily biologically degraded by laccase, so combination of enzyme and nanoscale Fe_3O_4 could be able to greatly improve the degradation rate of organochlorine pesticides. After oxidization by laccase, the intermediate 1-(2,2-dichloro-1-phenyl-ethyl)-4-methoxy-benzene (I) continued to be cleaved into 1-(2,2-dichloro-ethyl)-4-methoxy-benzene (*m*/*z* 205) fragment, which then carried out reductive cleavage to form methoxy-benzene (*m*/*z* 108) and 1,1-dichloroethane (*m*/*z* 98) under the action of USPIO (Majeau et al. 2010; Lei et al. 2003).

With the assistance by laccase, the generated methoxy-benzene underwent hydrogenation reduction and was turned into 1-methoxy-cyclohexene (*m*/*z* 112). According to Scourzic et al. (2015), the process of demethylation could occur under the action of enzymes. Therefore, 1-methoxy-cyclohexene could cause demethoxy reactions and form cyclohexene (*m*/*z* 82).

Magnetite is an inverse spinel crystal structure with a unit cell composed of 32 O^{2-} anions, 16 Fe^{3+} cations, and 8 Fe^{2+} cations, among them only Fe^{2+} cations can play a catalytic role for reduction. Fang et al. (2013) found that O_2 can readily accept electron from Fe(II) to produce $O_2{\cdot}^-$ and ·OH by electron paramagnetic resonance (EPR) technique determination, which have important implications for the degradation of organochlorine pesticide. In this paper, the particle size of USPIO is smaller than 12 nm; it could certainly cause quantum confinement effects (Vikesland et al. 2007) and greatly enhance the solid surface. So, quantum confinements can result in altering the surface free energy and the $O_2{\cdot}^-$ solvation shell, which may enhance the degradability of host/guest-type immobilized laccase (Furman et al. 2009). As a result, cyclohexene could be finally cleaved into vinyl, pentene, butane, and propane groups, as shown in Scheme 1 of Fig. 6.

Second, with the assistance by laccase, the intermediate cyclohexene and 1-(2, 2-dichloro-ethyl)-4-methoxy-benzene underwent hydrogenation reduction and changed to cyclohexane (II) and 4-(2,2-dichloro-ethyl)-1-methoxy-cyclohexene (IV), respectively. According to Zhai et al. (2001), methyl cyclopentane (III) should be the main pyrolysis product of cyclohexane (II) during the process of GC/MS analysis.

In the third degradation stage, cyclohexene was activated by $O_2{\cdot}^-$, to generate free radicals through the ring-opening reaction. By simultaneous action of immobilized laccase and reducing ferrous ion, the degradation products of 2-methylpentene (V) (*m*/*z* 84) could be obtained by free radical termination reaction, as shown in Scheme 3 of Fig. 6.

Mass spectrometry (GC/MS) of five degradation products can be seen in the Fig. S9a–d, and the mass spectra data based on the Fig. S9 after degradation of MXC can be seen in the Table 1, respectively.

As shown in Fig. S9 and Table 1, the product 1-(2,2-dichloro-1-phenyl-ethyl)-4-methoxy-benzene (I) showed a molecular peak at *m*/*z* 281 and displayed fragment ions at *m*/*z* 207($(M^+\text{-}C_6H_5)+2H^+$), 112($C_6H_5OCH_3+4H^+$), 98(CH_2CHCl_2), 83($(CH_3OC_4H_3)+H^+$), 70($CH_3OC_3H_3$), 57($CH_3OC_2H_2$), 41($(C_3H_2{}^+)+3H^+$), 31(CH_3O), and 28($C_2H_2+2H^+$). When one phenyl was cleaved from the degradation product (I) and the cleaving fragments continually obtained two protons, the fragment peak of *m*/*z* 207 could be observed. If this fragment proceeded with cleavage, the fragment peaks of *m*/*z* 112 and *m*/*z* 98 would be found. The former fragment *m*/*z* 112 continued to undergo cleavage to eliminate ethynyl group; as a result, two ion fragment peaks of *m*/*z* 83 and *m*/*z* 28 were obtained. Moreover, the former fragment *m*/*z* 112 could also eliminate cyclopropine (C_3H_2) by pyrolysis to form a molecular fragment peak of *m*/*z* 70 and an ion fragment peak of *m*/*z* 41. If the phenyl group was removed from the fragment *m*/*z* 112, the molecular fragment peak of 31 was obtained.

The reduction product cyclohexane (II) and its main pyrolysis product methyl cyclopentane (III) both showed a molecular peak at *m*/*z* 84 and displayed fragment ions at *m*/*z* 69 (C_5H_9), 56 (C_4H_8), 41($(C_3H_6)\text{-}H^+$), and 28(C_2H_4), respectively. During the pyrolysis process, part of cyclohexane (II) first changed into methyl cyclopentane (III), which could be demethylated to provide a fragment peak of *m*/*z* 69, but this fragment peak for cyclohexane (II) showed lower intensity than that for methyl cyclopentane (III), as shown in Table 1. Simultaneously, cyclohexane (II) and methyl cyclopentane (III) both underwent a cleavage for eliminating C_2H_4 and C_3H_6 groups to generate fragment peaks of *m*/*z* 56, 41, and 28, respectively.

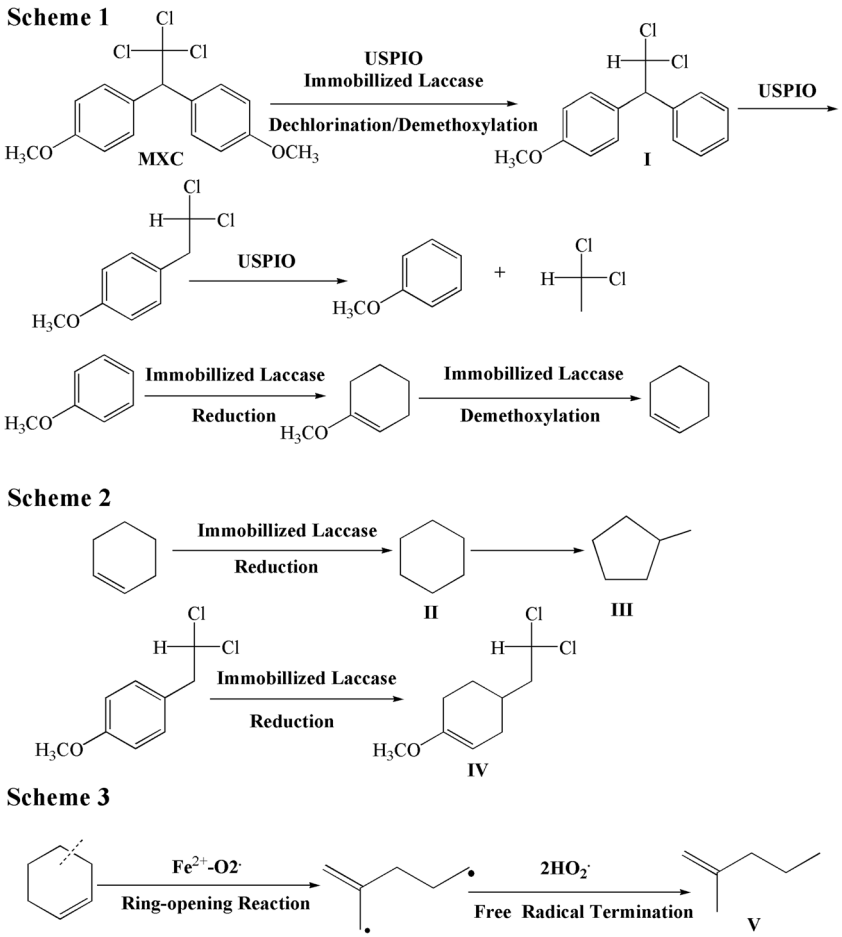

Fig. 6 Reaction mechanism of MXC degradation by laccase-MHGI

Another reduction product 4-(2,2-dichloro-ethyl)-1-methoxy-cyclohexene (IV) showed a molecular ion peak at *m/z* 211 ($M+2H^+$) and displayed fragment ions at *m/z* 184($(M-C_2H_4)+3H^+$), 112($(M-CH_2CHCl_2)+H^+$), 99($(CH_2CHCl_2)+H^+$), 83(C_5H_9O-$2H^+$), 70(C_4H_8O-$2H^+$), 57($C_4H_6+3H^+$), 41(C_3H_5), and 28(C_2H_4). When ethyl group was dissociated from the product (IV) by the ring-opening reaction of cyclohexene, an ion fragment peak of *m/z* 184 and a molecular fragment peak of *m/z* 28 were observed. A substituent group CH_2CHCl_2 could be dissociated from the product (IV) by cracking to provide two ion fragment peaks of *m/z* 112 and 99. If an ion fragment (peak of *m/z* 112) underwent a ring-opening reaction of cyclohexene to get rid of C_2H_4, an ion fragment peak of *m/z* 83 could be obtained. But, when the ion fragment (peak of *m/z* 112) underwent another ring-opening reaction of cyclohexene to get rid of C_3H_5, an ion fragment peak of *m/z* 70 and a molecular fragment peak of *m/z* 41 were observed. Besides, the presence of an ion fragment peak of *m/z* 57 could be obtained due to the dissociation of CH_3O from C_5H_9O.

The final degradation product 2-methyl pentene (V) showed a molecular peak at *m/z* 84 and displayed fragment ions at *m/z* 69(C_5H_9), 56($C_4H_7+H^+$), 41(C_3H_5), 27($C_2H_2+H^+$), and 15(CH_3). The peak at *m/z* 84 might be the molecular peak of 2-methyl pentene, and when methyl and methylene groups were dissociated from the product (V) in turn, molecular fragment peaks of *m/z* 69, 56, 41, and 15 were observed. Besides, the presence of an ion fragment peak of *m/z* 27 could be obtained due to the dissociation of CH_3 from allyl (C_3H_5) group.

In order to confirm the intermediates further, we also performed the ^1H NMR and ^{13}C NMR experiments. As the degraded products of MXC consisted of many ingredients, which were not easily separated and purified, and the quantities of the products were little, we conducted the NMR experiments for all of the degraded products. Based on the ^1H NMR and ^{13}C NMR spectra (ARX 600, Bruker, Germany), the results can be listed in Table 2.

All these results demonstrated the presence of 1-(2,2-dichloro-1-phenyl-ethyl)-4-methoxy-benzene, cyclohexane, 4-(2,2-dichloro-ethyl)-1-methoxy-cyclohexene, 2-methylpentene, and methyl cyclopentane in the degraded products, further demonstrating the possible MXC degradation reaction mechanism inferred in Fig. 6.

Conclusions

Taking SiO_2-TMs as carrier, laccase-MHGI was successfully synthesized with the method of co-adsorption and cross-linking, and the resulting composite material showed high stability and reusability as compared with the free laccase. The degradation of MXC was a first-order reaction, and activation energy of MXC degradation catalyzed by free laccase and immobilized laccase was 44.91 and 41.46 kJ mol^{-1}, respectively. Besides, 1-(2,2-dichloro-1-phenyl-ethyl)-4-methoxy-benzene, cyclohexane, 4-(2,2-dichloro-ethyl)-1-methoxy-cyclohexene, 2-methylpentene, and methyl cyclopentane were identified as the degradation products by GC/MS and NMR, and the degradation mechanism of MXC in water phase was also inferred accordingly.

Acknowledgments This work was supported by the National Natural Science Foundation of China (20577010, 20971043) and the Open Project Program of State Key Laboratory of Inorganic Synthesis and Preparative Chemistry, Jilin University.

References

Bourbonnais R, Paice MG (1992) Demethylation and delignification of kraft pulp by Trametes versicolor laccase in the presence of 2,2′-azinobis-(3-ethylbenzthiazoline-6-sulphonate). Appl Microbiol Biotechnol 36:823–827

Butt SB, Riaz M (2010) Radiolytic degradation of methoxychlor in methanol and monitoring of radiolytic products by HPLC and GC-MS. Radiochim Acta 98:307–314

Carvalho CML, Cabral JMS (2000) Reverse micelles as reaction media for lipases. Biochimie 82:1063–1085

Chen XC, Klingeler R, Kath M et al (2012) Magnetic silica nanotubes: synthesis, drug release, and feasibility for magnetic hyperthermia. ACS Appl Mater Interfaces 4:2303–2309

Dec J, Bollag JM (1994) Dehalogenation of chlorinated phenols during oxidative coupling. Environ Sci Technol 28:484–490

Deepthi SS, Prasad E, Reddy BVS et al (2014) A green approach towards the synthesis of enantio pure diols using horse radish peroxidase enzyme immobilized on magnetic nanoparticles. Green and Sustainable Chemistry 4:15–19

Duran N, Esposito E (2000) Potential applications of oxidative enzymes and phenoloxidase-like compounds in wastewater and soil treatment: a review. Appl Catal B Environ 28:83–99

Fang GD, Dionysiou DD, Al-Abed SR, Zhou DM (2013) Superoxide radical driving the activation of persulfate by magnetite nanoparticles: implications for the degradation of PCBs. Appl Catal B Environ 129:325–332

Furman O, Laine DF, Blumenfeld B et al (2009) Enhanced reactivity of superoxide in water-solid matrices. Environ Sci Technol 43:1528–1533

Garcia-Galan C, Berenguer-Murcia Á, Fernandez-Lafuente R et al (2011) Potential of different enzyme immobilization strategies to improve enzyme performance. Adv Synth Catal 353:2885–2904

Han PP, Jiang ZY, Wang XL et al (2015) Facile preparation of porous magnetic polydopamine microspheres through an inverse replication strategy for efficient enzyme immobilization. J Mater Chem B 3:7194–7202

Huang Y, Xi YJ, Yang YX et al (2014) Degradation of 2,4-dichlorophenol catalyzed by the immobilized laccase with the carrier of Fe_3O_4@MSS-NH_2. Chin Sci Bull 59:509–520

Hudson S, Cooney J, Magner E (2008) Proteins in mesoporous silicates. Angew Chem Int Ed 47:8582–8594

Ispas C, Sokolov I, Andreescu S (2009) Enzyme-functionalized mesoporous silica for bioanalytical applications. Anal Bioanal Chem 393:543–554

Jiang CN, Ling SM, Wang PF et al (2011) A new and sensitive catalytic resonance scattering spectral assay for the detection of laccase using guaiacol as substrate. Luminescence 26:500–505

Kimura M, Michizoe J, Oakazaki S et al (2004) Activation of lignin peroxidase in organic media by reversed micelles. Biotechnol Bioeng 88:495–501

Kouassi GK, Irudayaraj J, McCarty G (2005) Examination of cholesterol oxidase attachment to magnetic nanoparticles. J Nanobiotechnol 3:1–9

Lan J, Zhang Y, Huang XR et al (2008) Improvement of the catalytic performance of lignin peroxidase in reversed micelles. J Chem Technol Biotechnol 83:64–70

Lei LC, Shen XY, He F (2003) Mechanism of photo-Fenton degradation of ethanol and PVA. Chin J Chem Eng 11:577–582

Li YY, Qin C, Chen C et al (2012) Highly sensitive phenolic biosensor based on magnetic polydopamine-laccase-Fe3O4 bionanocomposite. Sensors Actuators B Chem 168:46–53

Luo X, Zhang L (2010) Immobilization of penicillin G acylase in epoxy-activated magnetic cellulose microspheres for improvement of biocatalytic stability and activities. Biomacromolecules 11:2896–2903

Majeau JA, Brar SK, Tyagi RD (2010) Laccases for removal of recalcitrant and emerging pollutants. Bioresour Technol 101:2331–2350

Martel S (2015) Magnetic nanoparticles in medical nanorobotics. J Nanoparticle Res 17:75

Netto CGCM, Toma HE, Andrade LH (2013) Superparamagnetic nanoparticles as versatile carriers and supporting materials for enzymes. J Mol Catal B Enzym 85–86:71–92

Scourzic L, Mouly E, Bernard OA (2015) TET proteins and the control of cytosine demethylation in cancer. Genome Med 7:9–24

Secundo F (2013) Conformational changes of enzymes upon immobilisation. Chem Soc Rev 42:6250–6261

Shao JG, Deng WJ, Yang YX et al (2009) Adsorption of laccase onto mesoporous silica prepared with inorganic counterions. Adsorpt Sci Technol 27:147–165

Šulek F, Fernández DP et al (2011) Immobilization of horseradish peroxidase as crosslinked enzyme aggregates (CLEAs). Process Biochem 46:765–769

Tavares APM, Silva CG et al (2015) Laccase immobilization over multiwalled carbon nanotubes: kinetic, thermodynamic and stability studies. J Colloid Interface Sci 454:52–60

Vikesland PJ, Heathcock AM, Rebodos RL et al (2007) Particle size and aggregation effects on magnetite reactivity toward carbon tetrachloride. Environ Sci Technol 41:5277–5283

Wang F, Huang W, Guo C, Liu CZ (2012) Functionalized magnetic mesoporous silica nanoparticles: fabrication, laccase adsorption performance and direct laccase capture from trametes versicolor fermentation broth. Bioresour Technol 126:117–122

Wang H, Li S, Si YM et al (2014) Recyclable enzyme mimic of cubic Fe_3O_4 nanoparticles loaded on graphene oxide-dispersed carbon nanotubes with enhanced peroxidase-like catalysis and electrocatalysis. J Mater Chem B 2:4442–4448

Wu ZC, Zhang B, Yan B (2009) Regulation of enzyme activity through interactions with nanoparticles. Int J Mol Sci 10:4198–4209

Yang YX, Wei QM, Zhang JB et al (2015) Degradation of MXC by host/guest-type immobilized laccase on magnetic tubular mesoporous silica. Biochem Eng J 97:111–118

Yu BB, Zeng JB, Lifen Gong LF et al (2007) Investigation of the photocatalytic degradation of organochlorine pesticides on a nano-TiO_2 coated film. Talanta 72:1667–1674

Zhai GH, Wang H, Yang HF et al (2001) Pyrolysis mechanism of cyclohexane (in Chinese). Acta Phys -Chim Sin 17:348–355

Zhang W, Huang X, Li Y et al (2006) Catalytic activity of lignin peroxidase and partitioning of veratryl alcohol in AOT/isooctane/water reverse micelles. Appl Microbiol Biotechnol 70:315–320